

A Possible Link Between Macroscopic Wear and Temperature Dependent Friction Behaviors of MoS₂ Coatings

Matthew A. Hamilton · Luis A. Alvarez · Nathan A. Mauntler ·
Nicolas Argibay · Rachel Colbert · David L. Burris · Chris Muratore ·
Andrey A. Voevodin · Scott S. Perry · W. Gregory Sawyer

Received: 1 February 2008 / Accepted: 18 September 2008
© Springer Science+Business Media, LLC 2008

Abstract Studies to explore the nature of friction, and in particular thermally activated friction in macroscopic tribology, have lead to a series of experiments on thin coatings of molybdenum disulfide. Coatings of predominately molybdenum disulfide were selected for these experiments; five different coatings were used: MoS₂/Ni, MoS₂/Ti, MoS₂/Sb₂O₃, MoS₂/C/Sb₂O₃, and MoS₂/Au/Sb₂O₃. The temperatures were varied over a range from -80 °C to 180 °C. The friction coefficients tended to increase with decreasing temperature. Activation energies were estimated to be between 2 and 10 kJ/mol from data fitting with an Arrhenius function. Subsequent room temperature wear rate measurements of these films under dry nitrogen conditions at ambient temperature demonstrated that the steady-state wear behavior of these coatings varied dramatically over a range of $K = 7 \times 10^{-6}$ to 2×10^{-8} mm³/(Nm). It was further shown that an inverse relationship between wear rate and the sensitivity of friction coefficient with temperature exists. The highest wear-rate coatings showed nearly athermal friction behavior, while the most wear resistant coatings showed thermally activated behavior. Finally, it is hypothesized that thermally activated behavior in macroscopic tribology is

reserved for systems with stable interfaces and ultra-low wear, and athermal behavior is characteristic to systems experiencing gross wear.

Keywords Solid lubrication · Molybdenum disulfide · Wear · Cryotribology

1 Introduction

There have been increasing efforts to measure and understand tribological behavior at cryogenic temperatures; to date, results of these efforts show either no trend or conflicting trends and often require cryogenic specific hypotheses. These measurements are difficult to make and often require sacrificing one or more experimental controls (e.g. dry sliding conditions, friction sensitivity, and background environment). Michael et al. [1], Theiler et al. [2], and Hubner et al. [3] compared results of ambient lab air testing with those of test submerged in cryogenic liquids and have shown either no trend or trends of reduced friction at cryogenic temperatures. Recent constant environment macroscale studies of various solid lubricants [4–7], and atomic-scale studies with terraces of graphite [8] show consistent trends of increased friction with decreased temperature, and the notion of thermally activated friction has been proposed [4, 8, 9]. Variable temperature experiments conducted on beds of aligned carbon nanotubes [10] and various high temperature polymer studies [11–16] have also demonstrated behavior that is well fit by an activated process at the macroscale. Burton et al. [17] found inconclusive trends during tilted sled experiments with sapphire, PTFE, and other materials over a range of 4–400 K under dry sliding in vacuum but notes that “...we believe that the effects of wear overwhelm any possible temperature

M. A. Hamilton · L. A. Alvarez · N. A. Mauntler · N. Argibay ·
R. Colbert · D. L. Burris · W. G. Sawyer (✉)
Department of Mechanical and Aerospace Engineering,
University of Florida, Gainesville, FL 32611, USA
e-mail: wgsawyer@ufl.edu

S. S. Perry · W. G. Sawyer
Department of Materials Science and Engineering, University
of Florida, Gainesville, FL 32611, USA

C. Muratore · A. A. Voevodin
Wright Laboratory, Materials Directorate, Wright Patterson Air
Force Base, Dayton, OH 45433, USA

dependent friction mechanisms.” We hypothesize that under conditions of significant wear, friction coefficients are insensitive to temperature because the systems are not sliding along stable interfaces. When wear is minor, the friction is strongly dependent on the contacting surfaces’ local atomic and molecular level termination. Here, we revisit the earlier experimental setup to perform macroscopic variable temperature experiments on a suite of molybdenum disulfide coatings.

Due to water adsorption and frost, macroscopic measurements of friction coefficient in cryogenic temperature ranges requires that experiments are performed in either vacuum or a gas environment with very little water vapor (this was discussed and demonstrated in detail by Burris et al. [4]). Clean graphitic terraces provide model surfaces on which to perform nanotribology measurements, but they suffer from high wear in the dry environments necessary for cryogenic experiments. Molybdenum disulfide films are well suited and have a long history of successful operation in inert and dry environments [18–24]. As such they are ideal candidates for these experiments. The experiments reported here complement the previous experiments performed on PTFE and demonstrate the existence of thermally activated behavior for thin coatings that do not have the viscoelastic behavior that PTFE often exhibits.

2 Variable Temperature Experimental Setup with MoS₂ Coatings

The molybdenum disulfide coatings selected for this effort are more fully described in Sect. 3. Briefly, they are all thin films and are described by their constituents: MoS₂/Ni, MoS₂/Ti, MoS₂/Sb₂O₃, MoS₂/C/Sb₂O₃, and MoS₂/Au/Sb₂O₃. The coatings are typically a few micrometers thick, and were applied on aluminum 7075-T6 substrates and pins. All experiments were run under self-mated conditions.

The variable temperature experiments followed the experimental approach discussed by McCook et al. [5] and used a rotating pin-on-disk tribometer with impinging jets of dry nitrogen that blanketed the disk’s surface. The temperature of the disk surface is prescribed by mixing various amounts of liquid nitrogen into the impinging jet. The liquid nitrogen volatilizes prior to arrival at the disk surface. Experiments and discussion in Burris et al. [4] suggest that this technique is likely free of frost down to approximately –100 °C.

Figure 1 shows a plot that is produced at the end of four experimental runs on self-mated MoS₂/C/Sb₂O₃ coatings. Each experimental run uses a unique location on the pin surface (six locations can be run per pin sample) and a unique location on the disk surface. The sliding speeds are

maintained at 10 mm/s for each experimental run and the normal load is held at 5 N via a dead-weight load. The data span a temperature range from approximately –80 °C to 180 °C in four distinct bins. The vertical line of data at 27.3 °C is collected in the nitrogen gas environment with no forced nitrogen flow. The open triangles represent the average temperature and average friction coefficient recorded during steady operation. The confidence intervals represent a standard deviation of this selected data and overlays the plot in this region. Four such computations are made for each sample. The plot in Fig. 1 shows all of the data including transient behavior that is excluded from the averages. At the conclusion of the ambient temperature run, a new location on the pin and disk are selected, speeds and loads are set, and the surface temperature is either elevated or lowered from this point. The data at 173 °C shows the long transients observed during warming of the surface as well as the rapid transient during cooling; the average values represent approximately 30 min of continuous operation around the 170 °C point. The third experimental run begins at a targeted subambient temperature of approximately –20 °C. After 50 m of sliding, the temperature is further cooled to a target temperature of approximately –80 °C where it is held for approximately 2,000 s before being gently warmed back up to –20 °C. The inset graph in the top right plots both the surface temperature and the friction coefficient versus time (or sliding distance) during the transition from –20 °C to –80 °C. The transitions in temperature are on the order of 2 °C per minute and the friction coefficient follows the temperature changes closely. This experimental process is repeated for each of the coatings with average values being collected for four temperatures over the range of –80–180 °C.

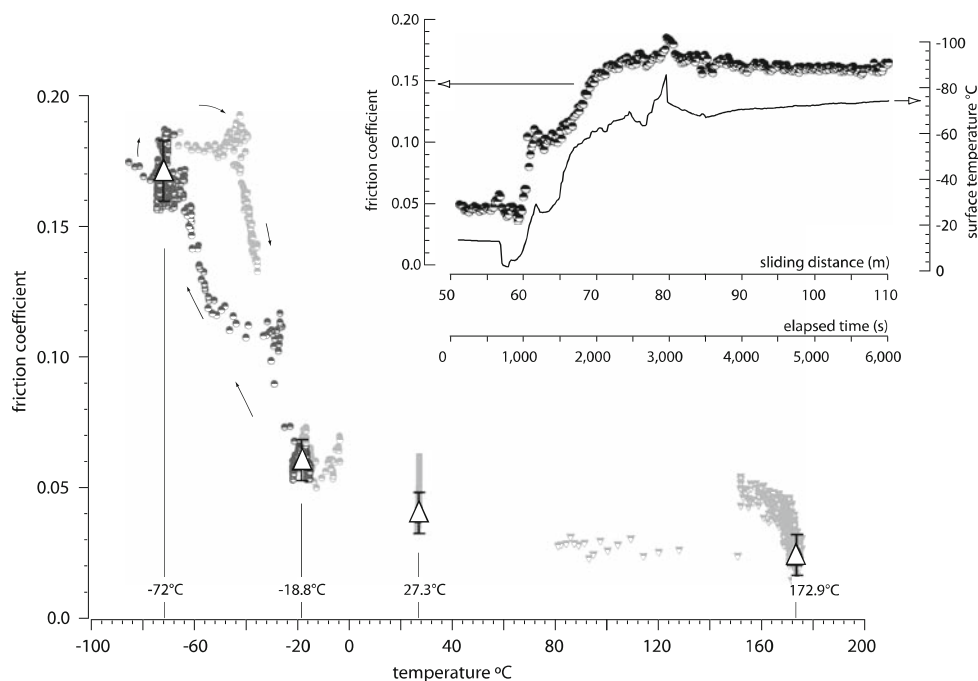
3 Methods

3.1 Molybdenum Disulfide Coatings

All coatings were deposited on aluminum 7075-T6 materials for the variable temperature rotating pin-on-disk experiments. Later coatings were deposited on 304 Stainless Steel for the reciprocating pin-on-disk experiments performed under the scanning-white-light-interferometer. All experiments were run self-mated and the corresponding pins were of the same material and were 6.35 mm in diameter.

MoS₂/Ni: This coating was made by Dayton Coating Technologies via a DC magnetron sputtering route. The coating is approximately 95% MoS₂ and 5% Ni by weight, as reported by the manufacturer.

Fig. 1 The plot shows friction coefficient versus the measured surface disk temperature of the disk sample for a self-mated MoS₂/C/Sb₂O₃ coating. Three wear tracks were run on this sample as illustrated by the circular, triangular, and square data points (which appear as a vertical line at 27.3 °C). The data include transient behaviors with the progression of time indicated by the arrows. From this data, four datum points are collected at the temperatures indicated on the bottom of the graph and shown overlaid on the plot as open triangles. The inset graph plots the transition behavior from roughly -20 °C to -70 °C for the darkened points on the left of the primary graph



MoS₂/Ti: This coating was made by Teer Coatings LTD via an unbalanced DC magnetron sputtering route with MoS₂ and Ti targets. It is reported by the manufacturer to be a multi-layered coating with layer thickness on the order of 100–200 nm. It is reportedly 15% Ti by weight.

MoS₂/Au/Sb₂O₃: This coating was DC sputtered by Hohman Plating from a composite target.

MoS₂/C/Sb₂O₃: This coating was deposited by the AFRL using a pulsed laser deposition process from a single composite target of molybdenum disulfide, graphite, and antimony trioxide. The weight percents are 50% molybdenum disulfide, 30% antimony trioxide, and the remainder is graphite.

MoS₂/Sb₂O₃: This coating was deposited by the AFRL using a pulsed laser deposition process from a single composite target of molybdenum disulfide and antimony trioxide, with weight percents of 70% and 30%, respectively.

3.2 Variable Temperature Environment Details

The experimental setup and environment are described by McCook et al. [5]. Here the thermocouple used for reading the disk surface temperature is mounted directly to the tribometer and is mechanically held in a sliding contact for the duration of the test. All temperatures reported in this study are from this thermocouple. The nitrogen delivery system consists of an impinging jet of dry nitrogen that is cooled and used to evaporate the liquid nitrogen impinging jet. This dry nitrogen is passed through a tube heat exchanger that is submerged in a frozen slush of isopropyl

alcohol at ~ -130 °C. Thermal control was achieved by varying flow rates of the liquid and dry nitrogen until a steady and targeted surface temperature was achieved.

3.3 Reciprocating Tribometer Instrumentation

The stage on the reciprocating tribometer is driven by a stepper motor, and has a linear position accuracy of 10 μm , and a repeatability of ± 1.3 μm . A BEI encoder (model 27A383) combined with a Renishaw optical encoder read-head (model RGH24Z) sends position data from the linear stage to the DAQ, with a resolution of 0.5 μm . Normal and friction forces are measured using a JR3 6 channel load cell (model 20E12A4-I25-E 25L50), with an approximate uncertainty of 30 mN on each of the two channels used (normal force and friction force). Relative humidity was measured using a GE HygroGuard (model MMY 2650) hygrometer with a DY 5-series probe, with an accuracy of 0.1% relative humidity. Ambient temperature was measured using an Omega digital thermo-hygrometer (model RH411), with an accuracy of 0.5 °C. The local sample surface temperature was measured using an Omega temperature controller (model CNI3252) connected to an Omega unshielded K-type thermocouple, with an overall accuracy of 0.5 °C. The thermocouple tip was sandwiched between the sample and one of the four clamping screws on the corners of the sample, ensuring a solid mechanical contact between the sample and thermocouple. The oxygen level in the environment chamber was measured using a Delta F oxygen sensor (model 310E) with an accuracy of approximately 0.2 ppm of O₂.

3.4 Reciprocating Tribometer Operation

After mounting the pin and counterface sample to the tribometer, the environment chamber is assembled. Once the environmental conditions have been adjusted to the appropriate levels, an initial measurement of the sample surface is performed at some point of interest in the projected wear track. Typically, surface measurements are recorded as the average of five repeated interferometer scans to reduce noise. Additionally, best fit plane and position offsets are removed to facilitate comparisons with subsequent measurements.

Following the initial surface measurement, the stage is positioned beneath the pin where the normal load is applied via the vertical micrometer stage. As the load is applied, leaf-type flexures maintain alignment of the load cell axes with the counterface. Half, single, or multiple reciprocations of the stage are then carried out while recording load and position. The sample is then unloaded and repositioned beneath the interferometer objective in the same location as the original surface scan and the worn surface is measured. By repeating the process of scanning the surface following reciprocation testing, friction force data can be directly related to surface wearing events as the test progresses.

3.5 Data Acquisition

A National Instruments 6014 E PCI card and an SCB-68 data acquisition board (DAQ) were used as the interface between the various hardware components and the analysis and control software, which was custom made in LabVIEW for this specific application. The LabVIEW software was set to acquire 1,000 data points per second (1,000 Hz) for each of the input channels. The input signals are all analog 0–10 VDC, which are digitized by the DAQ and interpreted with calibration equations provided by the respective instrument manufacturers. Any initial offsets encountered in the force measurements are removed using a software zero prior to initial loading of the pin onto the counterface.

4 Results of Variable Temperature Experiments

The average friction coefficients for the five unique MoS₂ coatings are shown for four temperatures over the range of –80–180 °C in Fig. 2. Table 1 gives the average values for each of the coatings. The data show a general trend of increased friction with decreased temperature, and although the sensitivity to temperature varied from sample to sample, all of the coatings exhibited higher friction at the coldest temperature when compared to the warmest temperature. One striking observation is that the coating with

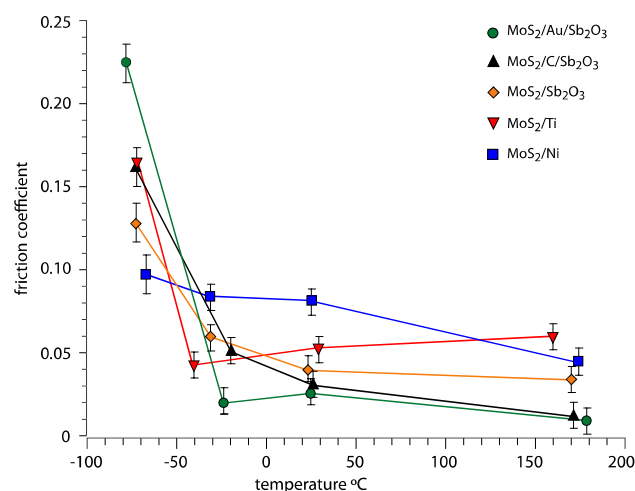


Fig. 2 Average friction coefficients are plotted versus temperatures from roughly –80 °C to 180 °C for five different self-mated molybdenum disulfide coatings. All experiments were run under an impinging jet of dry nitrogen. The data are supplied in Table 1

the highest friction coefficient under ambient conditions had the lowest friction coefficient at cryogenic conditions; the obverse trend is also observed with the lowest friction coating at ambient having the highest at cryogenic temperatures.

It is well known that the shear stress of viscous lubricants increases with shear rate and temperature; Michael et al. [9] found strong evidence of thermally activated shear strength and friction with fatty acid boundary lubricated copper; these results were largely discussed in the context of viscosity. The same trend has been observed in the polymer tribology literature for more than 50 years [13–16] and the behavior is often attributed to viscoelasticity. Here, we find evidence of the same characteristics in a material that exhibits velocity independence or ‘negatively’ sloped friction–velocity dependences, suggesting a more general phenomenon of slip occurring through thermally activated processes. In the envisaged model, thermal energy promotes an aggregation of atomic slip events from one stable state to the next that is detectable through macroscopic friction measurements of very stable interfaces.

Assuming thermally activated friction behavior, activation energies and reference friction coefficients are found through curve fitting the data using Eq. 1 following an approach that is outlined in McCook et al. [5]. The free parameters in the curve fitting activity are a reference friction coefficient μ_0 and the activation energy E_a ; the reference temperature is set at $T_0 = 300$ K.

$$\mu = \mu_0 e^{\left(\frac{-E_a}{R} \left(\frac{1}{T_0} - \frac{1}{T}\right)\right)} \quad (1)$$

The coatings are listed from highest activation energy to lowest in Table 1. Interestingly the coatings are also ranked

Table 1 Results of variable temperature tribology studies of five coatings containing primarily MoS₂: friction coefficients for varying test temperature, activation energy calculations from fits of variable temperature friction data assuming thermally activated behavior and wear rates, and uncertainties in wear rate at room temperature

	Temperature (°C)	μ	Ea (kJ/mol)	μ_0	$K/u(K)$
MoS ₂ /Au/Sb ₂ O ₃	-77.2	0.228	9.8	0.027	$K = 1.9 \times 10^{-8} \text{ mm}^3/\text{N-m}$ $u(K) = 0.6 \times 10^{-8} \text{ mm}^3/\text{N-m}$
	-23.6	0.022			
	26.3	0.028			
	180.7	0.011			
MoS ₂ /C/Sb ₂ O ₃	-72.0	0.166	8.0	0.034	$K = 2.3 \times 10^{-8} \text{ mm}^3/\text{N-m}$ $u(K) = 0.4 \times 10^{-8} \text{ mm}^3/\text{N-m}$
	-18.8	0.054			
	27.3	0.034			
	172.9	0.015			
MoS ₂ /Sb ₂ O ₃	-72.2	0.131	5.7	0.042	$K = 5.3 \times 10^{-7} \text{ mm}^3/\text{N-m}$ $u(K) = 0.2 \times 10^{-7} \text{ mm}^3/\text{N-m}$
	-30.3	0.063			
	24.6	0.043			
	172.1	0.037			
MoS ₂ /Ti	-71.4	0.133	5.2	0.056	$K = 7.2 \times 10^{-7} \text{ mm}^3/\text{N-m}$ $u(K) = 1.0 \times 10^{-7} \text{ mm}^3/\text{N-m}$
	-39.8	0.010			
	30.5	0.055			
	161.8	0.076			
MoS ₂ /Ni	-66.0	0.100	2.6	0.067	$K = 7.4 \times 10^{-6} \text{ mm}^3/\text{N-m}$ $u(K) = 1.1 \times 10^{-6} \text{ mm}^3/\text{N-m}$
	-30.2	0.087			
	26.8	0.084			
	176.0	0.047			

inversely with friction coefficient at ambient temperatures—the higher the ambient friction coefficient of the coatings the lower the activation energy. Qualitatively, the coatings with low friction coefficient at ambient temperature were observed to be much more wear resistant than the others. Unfortunately no quantitative measurements of the steady-state wear rates could be made from the variable temperature pin-on-disk experiments.

5 Measurements of Steady-State Wear Rates in MoS₂ Coatings

The hypothesis derived from the variable temperature experiments is that higher wear rates lead to reduced sensitivity of friction coefficient to temperature. The highest quality coatings are those that have both low friction and low wear; it was these coatings that appeared to be most affected by changes in temperature. In order to measure the wear-rates of these films during operation in a dry nitrogen environment, a unique tribometer that could make direct surface topographic measurements without removing the samples from the environment was constructed. This apparatus is shown schematically in Fig. 3. Briefly, the reciprocating pin-on-disk tribometer

uses a multiaxial load cell located in the force path to ground and rigidly attached to the stationary pin. This follows the methodology analyzed in a paper by Schmitz et al. [25] that discusses the difficulty of making low friction coefficient measurements. Unique to this tribometer is the ability to position and stop the disk sample under a scanning white-light interferometer objective and perform repeated surface scans on the same location of the wear track during sliding. This feature enables incremental measurements of wear to be monitored and measured during operation without breaking the gas environment.

For this study, coatings were deposited on 304 stainless steel spheres and rectangular flat samples. The experiments were run in a dry nitrogen environment at ambient temperature under a 5 N load and 10 mm/s sliding speed. Experiments were run for 10,000 cycles and wear measurements were made incrementally every 1,000 cycles. Fitting these data using a Monte Carlo technique (described in a paper on wear rate uncertainty analysis by Schmitz et al. [26]) gives steady-state wear-rate, K , and associated uncertainties, $u(K)$. A wide range of wear-rates was observed in these coatings (from a high of $K = 7 \times 10^{-6}$ to a low of $K = 2 \times 10^{-8} \text{ mm}^3/(\text{Nm})$). The data are given in Table 1.

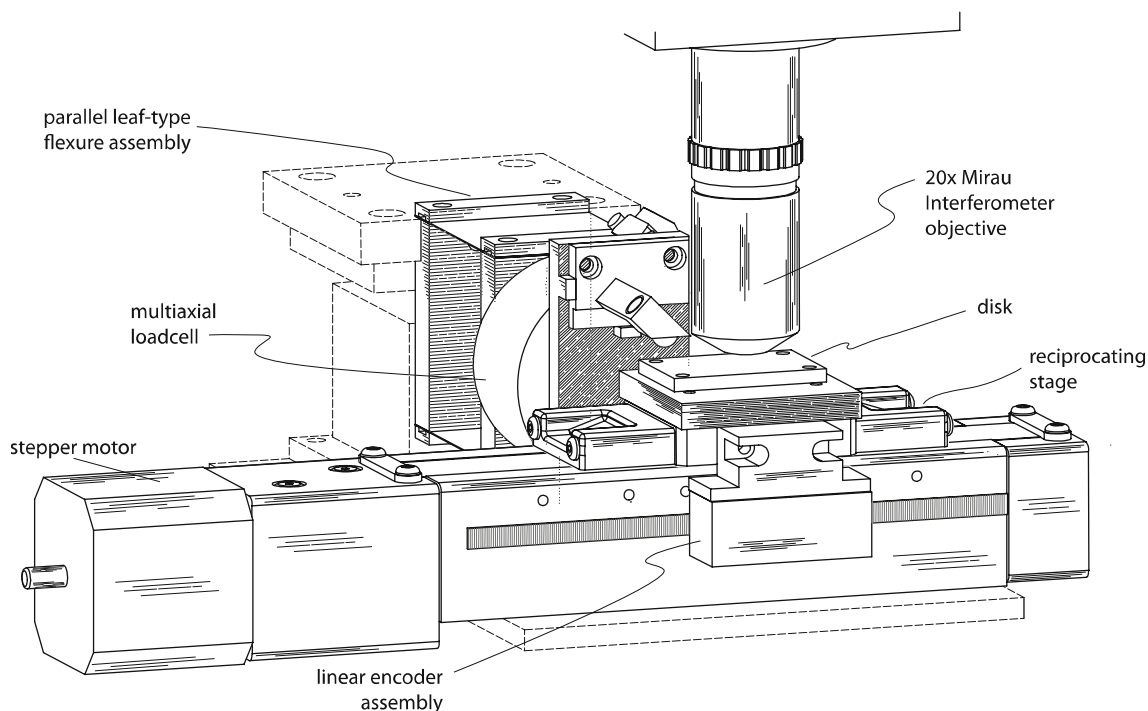


Fig. 3 A schematic of the reciprocating pin-on-disk tribometer that was constructed under a scanning white-light interferometer and used to measure the wear rates of the self-mated molybdenum disulfide films. The tribometer uses a parallel leaf-type flexure assembly to

impose a normal load. All of the normal and frictional forces are measured using a multi-axial load-cell that is rigidly mounted to the pin sample. The stage and stepper motor assembly is used to position the sample under the microscope objective

6 Discussion

Figure 4 shows an inverse relationship between the activation energy and wear rate (measured at room temperature). This suggests that the components of friction force associated with wear and wear debris can be larger than those related to thermally activated slip and under conditions of gross wear thermally activated behavior may be suppressed. Friction coefficient and Arrhenius plots are also shown for the most thermally sensitive and thermally insensitive samples. The variations in the behaviors and the fluctuations in the friction coefficients may be a result of sample to sample variations, variation in wear rate, and the stochastic nature of wear and its contributions to friction forces. It should be noted that during single experiments, friction was never directly observed to decrease during temperature reductions.

The relationship between athermal friction processes and wear may not be that surprising for systems that experience gross plastic deformation, because relatively simple friction models predict no relationship between friction coefficient and material properties such as hardness, yield strength, or elastic modulus. In macroscopic models for friction that follow classical mechanics approaches [27] there are no considerations for

corrugations in a surface potential or energetic barriers to sliding; rather, these models compute or analyze continuum level deformations and geometric considerations of the surface topography in an effort to describe frictional behavior.

In this study 5 very different films of predominately MoS_2 were interrogated in an environment that promotes low friction and wear. Current hypotheses of MoS_2 lubrication suggest that molecularly thin films are sufficient for low friction [28]. At wear rates of $1 \times 10^{-7} \text{ mm}^3/(\text{Nm})$, wear of the MoS_2 is occurring at less than a monolayer per pass; thus, the prevailing model for these experiments on the low wear coatings is that the layered MoS_2 persists for a number of cycles before being removed for another layer of MoS_2 . The relationship between the activation energy and wear rate is striking—the higher the wear rate the lower the activation energy. Detailed examination of films at opposite ends of the wear and friction behavior is particularly revealing. The $\text{MoS}_2/\text{C}/\text{Sb}_2\text{O}_3$ and MoS_2/Ni samples had differences in wear rate over $100\times$ and the friction coefficient trend with temperature for the high wear MoS_2/Ni sample only varied by a factor of two over the 250°C temperature range. Previous studies of the $\text{MoS}_2/\text{C}/\text{Sb}_2\text{O}_3$ composite coatings in dry nitrogen sliding have shown that they

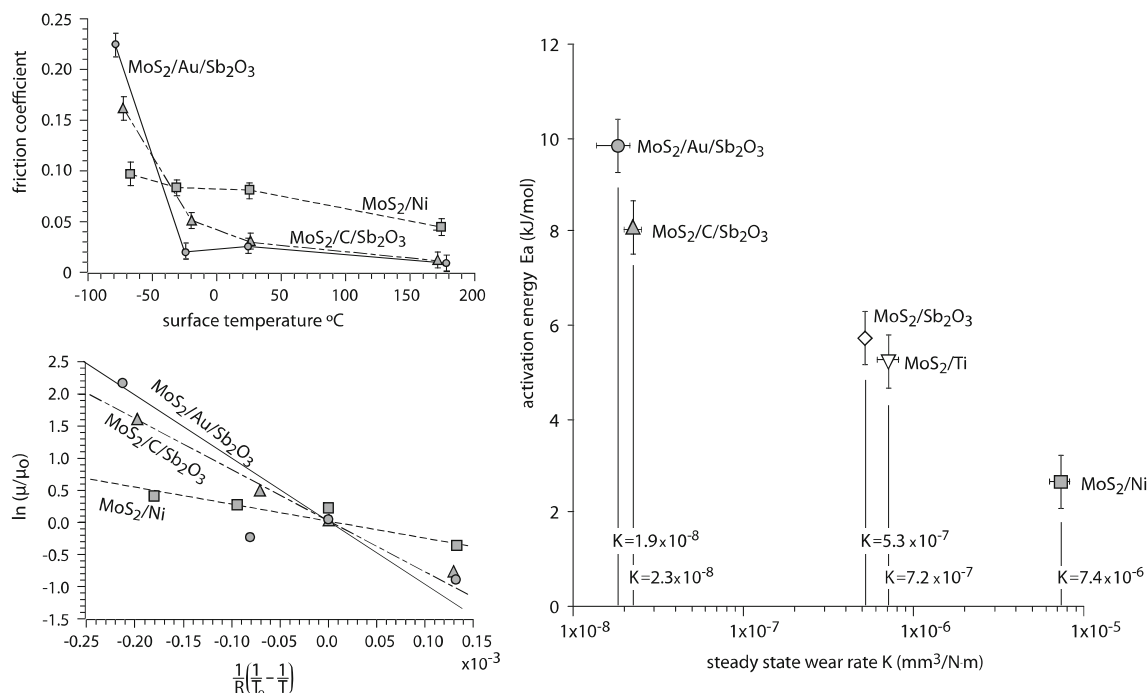


Fig. 4 The graph on the right plots the curve fit values of activation energy versus the steady-state wear rate of the five coatings. The higher wear rate films showed a behavior that had a lesser dependence on temperature. This nearly athermal behavior of friction coefficient is exemplified in the graphs on the left which contrast the behavior

between the two materials with the lowest wear rates and the material with the largest wear rate. The top graph compares the material's friction coefficients, while the bottom graph displays the activation energy as the slopes of the data's curve fits. The materials, wear rates, and associated uncertainties are given in Table 1

develop a thin layer of MoS₂ basal planes oriented parallel to the surfaces during running-in, after which the wear process is a minimum [29]. The established interfacial surfaces relative motion is then likely governed by surface potential interactions of MoS₂ sliding against itself. Coatings with the capability to form stable velocity accommodating interfaces may then show strong temperature dependence, with friction coefficient going up rapidly at cryogenic temperatures. The higher friction coefficient at room temperature for the high wear film is consistent with the hypothesis of wear dominating the velocity accommodation. It is interesting that around $-50\text{ }^{\circ}\text{C}$ a crossover in friction coefficient occurs—the friction coefficient of the low wear coating now exceeds the friction coefficient of the high wear coating.

Although potentially premature without wear-rate measurements at cryogenic temperatures, the model suggested by these experiments is that under conditions of gross wear, the friction coefficient is independent of temperature; it is only under conditions of extremely low wear that the interfaces are stable enough that surface potentials are the dominant energetic barriers to sliding. As the size scale approaches the macroscale, gross wear becomes more likely and the detection of thermally activated behavior less likely. In systems that are low wear and thought to have

interfacial sliding in macroscopic experiments monotonic temperature dependences in the direction of increasing friction coefficient with decreasing temperature have been observed. Fits to activation energy give values between 2 and 12 kJ/mol [4, 5, 10].

7 Concluding Remarks

Friction coefficients of MoS₂ coatings increased with decreasing temperature over a range from roughly $-80\text{ }^{\circ}\text{C}$ to $180\text{ }^{\circ}\text{C}$. These coatings had wear rates from a high of $K = 7 \times 10^{-6}$ to a low of $K = 2 \times 10^{-8}$ mm³/(Nm), and the coatings with the highest wear rates had friction behavior that was only weakly dependent on temperature and low wear samples showed a strong friction dependence on temperature. Detailed investigation of the steady-state wear-rates of the lowest wear coatings indicates that the wear mechanism is very gradual and suggests that a single MoS₂ layer likely persists for a number of cycles. It is hypothesized that athermal behavior is characteristic of systems experiencing gross wear. In macroscopic tribology, thermally activated behavior is reserved for systems with stable interfaces and ultra-low wear.

Acknowledgements This material is supported by an AFOSR-MURI grant FA9550-04-1-0367. Any opinions, findings, and conclusions or recommendations expressed in this material are those of the authors and do not necessarily reflect the views of the Air Force Office of Scientific Research. The authors would also like to thank Profs. Tony Schmitz and John Ziegert for their help in designing the reciprocating tribometer used in this study.

References

- Michael, P., Rabinowicz, E., Iwasa, Y.: Friction and wear of polymeric materials at 293-k, 77-k and 4.2-k. *Cryogenics* **31**, 695–704 (1991). doi:[10.1016/0011-2275\(91\)90230-T](https://doi.org/10.1016/0011-2275(91)90230-T)
- Theiler, G., Hubner, W., Gradt, T., Klein, P., Friedrich, K.: Friction and wear of ptfe composites at cryogenic temperatures. *Tribol. Int.* **35**, 449–458 (2002). doi:[10.1016/S0301-679X\(02\)0035-X](https://doi.org/10.1016/S0301-679X(02)0035-X)
- Hubner, W., Gradt, T., Schneider, T., Borner, H.: Tribological behaviour of materials at cryogenic temperatures. *Wear* **216**, 150–159 (1998). doi:[10.1016/S0043-1648\(97\)00187-7](https://doi.org/10.1016/S0043-1648(97)00187-7)
- Burris, D.L., Perry, S.S., Sawyer, W.G.: Macroscopic evidence of thermally activated friction with polytetrafluoroethylene. *Tribol. Lett.* **27**, 323–328 (2007). doi:[10.1007/s11249-007-9237-6](https://doi.org/10.1007/s11249-007-9237-6)
- McCook, N.L., Burris, D.L., Dickrell, P.L., Sawyer, W.G.: Cryogenic friction behavior of ptfe based solid lubricant composites. *Tribol. Lett.* **20**, 109–113 (2005). doi:[10.1007/s11249-005-8300-4](https://doi.org/10.1007/s11249-005-8300-4)
- Ostrovskaya, Y., Yuhno, T., Gamulya, G., Vvedenskij, Y., Kuleba, V.: Low temperature tribology at the b. Verkin institute for low temperature physics & engineering (historical review). *Tribol. Int.* **34**, 265–276 (2001). doi:[10.1016/S0301-679X\(01\)0010-X](https://doi.org/10.1016/S0301-679X(01)0010-X)
- Yuhno, T.P., Vvedensky, Y.V., Sentyurikhina, L.N.: Low temperature investigations on frictional behaviour and wear resistance of solid lubricant coatings. *Tribol. Int.* **34**, 293–298 (2001). doi:[10.1016/S0301-679X\(01\)00013-5](https://doi.org/10.1016/S0301-679X(01)00013-5)
- Zhao, X., Hamilton, M., Sawyer, W.G., Perry, S.S.: Thermally activated friction. *Tribol. Lett.* **27**, 113–117 (2007)
- Michael, P.C., Rabinowicz, E., Iwasa, Y.: Thermal activation in boundary lubricated friction. *Wear* **193**, 218–225 (1996). doi:[10.1016/0043-1648\(95\)06722-1](https://doi.org/10.1016/0043-1648(95)06722-1)
- Dickrell, P.L., Pal, S.K., Bourne, G.R., Muratore, C., Voevodin, A.A., Ajayan, P.M., et al.: Tunable friction behavior of oriented carbon nanotube films. *Tribol. Lett.* **24**, 85–90 (2006). doi:[10.1007/s11249-006-9162-0](https://doi.org/10.1007/s11249-006-9162-0)
- Friedrich, K., Kargerkocsis, J., Lu, Z.: Effects of steel counterface roughness and temperature on the friction and wear of pe(e)k composites under dry sliding conditions. *Wear* **148**, 235–247 (1991). doi:[10.1016/0043-1648\(91\)90287-5](https://doi.org/10.1016/0043-1648(91)90287-5)
- Pleskachevsky, Y.M., Smurugov, V.A.: Thermal fluctuations of ptfe friction and transfer. *Wear* **209**, 123–127 (1997). doi:[10.1016/S0043-1648\(97\)00034-3](https://doi.org/10.1016/S0043-1648(97)00034-3)
- Blanchet, T., Kennedy, F.: Sliding wear mechanism of polytetrafluoroethylene (ptfe) and ptfe composites. *Wear* **153**, 229–243 (1992). doi:[10.1016/0043-1648\(92\)90271-9](https://doi.org/10.1016/0043-1648(92)90271-9)
- McLaren, K., Tabor, D.: Visco-elastic properties and friction of solids—friction of polymers—influence of speed and temperature. *Nature* **197**, 856–858 (1963)
- Pooley, C.M., Tabor, D.: Friction and molecular structure—behavior of some thermoplastics. *Proc. R. Soc. Lond. A-Math Phys. Sci.* **329**, 251–274 (1972)
- Tanaka, K., Uchiyama, Y., Toyooka, S.: Mechanism of wear of poytetrafluoroethylene. *Wear* **23**, 153–172 (1973). doi:[10.1016/0043-1648\(73\)90081-1](https://doi.org/10.1016/0043-1648(73)90081-1)
- Burton, J., Taborek, P., Rutledge, J.: Temperature dependence of friction under cryogenic conditions in vacuum. *Tribol. Lett.* **23**, 131–137 (2006). doi:[10.1007/s11249-006-9115-7](https://doi.org/10.1007/s11249-006-9115-7)
- Dvorak, S.D., Wahl, K.J., Singer, I.L.: In situ analysis of third body contributions to sliding friction of a pb-mo-s coating in dry and humid air. *Tribol. Lett.* **28**, 263–274 (2007). doi:[10.1007/s11249-007-9270-5](https://doi.org/10.1007/s11249-007-9270-5)
- Haltner, A.J., Oliver, C.S.: Effect of water vapor on friction of molybdenum disulfide. *Ind Eng Chem Fundam* **5**, 348–355 (1966)
- Lavik, M., Haltner, A.J., Spalvins, T.: Discussion of deposition of mos2 films by physical sputtering and their lubrication properties in vacuum. *Asle Trans.* **12**, 41 (1969)
- Voevodin, A.A., Fitz, T.A., Hu, J.J., Zabinski, J.S.: Nanocomposite tribological coatings with “Chameleon” surface adaptation. *J. Vac. Sci. Technol. A* **20**, 1434–1444 (2002)
- Voevodin, A.A., Zabinski, J.S.: Nanocomposite and nanostructured tribological materials for space applications. *Compos. Sci. Technol.* **65**, 741–748 (2005)
- Voevodin, A.A., Zabinski, J.S., Muratore, C.: Recent advances in hard, tough, and low friction nanocomposite coatings. *Tsinghua Sci. Technol.* **10**, 665–679 (2005). doi:[10.1016/S1007-0214\(05\)70135-8](https://doi.org/10.1016/S1007-0214(05)70135-8)
- Zabinski, J.S., Donley, M.S., Walck, S.D., Schneider, T.R., Mcdevitt, N.T.: The effects of dopants on the chemistry and tribology of sputter-deposited mos2 films. *Tribol. Trans.* **38**, 894–904 (1995). doi:[10.1080/10402009508983486](https://doi.org/10.1080/10402009508983486)
- Schmitz, T., Action, J., Ziegert, J., Sawyer, W.: The difficulty of measuring low friction: uncertainty analysis for friction coefficient measurements. *Tribol. Trans.* **127**, 673–678 (2005). doi:[10.1115/1.1843853](https://doi.org/10.1115/1.1843853)
- Schmitz, T., Action, J., Burris, D., Ziegert, J., Sawyer, W.: Wear-rate uncertainty analysis. *J Tribol-Trans Asme* **126**, 802–808 (2004). doi:[10.1115/1.1792675](https://doi.org/10.1115/1.1792675)
- Williams, J.: *Engineering tribology*, p. 488. Oxford University Press, Oxford, New York (1994)
- Wahl, K.J., Dunn, D.N., Singer, I.L.: Wear behavior of pb-mo-s solid lubricating coatings. *Wear* **230**, 175–183 (1999). doi:[10.1016/S0043-1648\(99\)00100-3](https://doi.org/10.1016/S0043-1648(99)00100-3)
- Zabinski, J.S., Bultman, J.E., Sanders, J.H., Hu, J.J.: Multi-environmental lubrication performance and lubrication mechanism of mos2/sb2o3/c composite films. *Tribol. Lett.* **23**, 155–163 (2006). doi:[10.1007/s11249-006-9057-0](https://doi.org/10.1007/s11249-006-9057-0)